

A. Azens · C.G. Granqvist

## Electrochromic smart windows: energy efficiency and device aspects

Received: 26 September 2001 / Accepted: 17 December 2001 / Published online: 26 September 2002  
© Springer-Verlag 2002

**Abstract** This paper covers three aspects of electrochromic smart windows. Their energy efficiency is discussed, and it is argued that a control strategy considering whether a room is in use or not can lead to large savings of the energy needed for space cooling. With regard to durability, it is shown that chemical compatibility between the electrolyte and electrochromic films of tungsten oxide and nickel oxide can be achieved without loss of optical transparency. Finally, we consider device manufacturability and present data on precharging of electrochromic nickel oxide films by ozone treatment.

**Keywords** Electrochromism · Thin films · Tungsten oxide · Nickel oxide · Smart windows

### Introduction

Intelligent glass façades [1] and smart windows [2] are attracting much interest in contemporary architecture. These windows are characterized by their ability to modulate the throughput of light and solar energy. Electrochromism [2] is a well-known phenomenon capable of providing the required variation in the optical properties, and presently some full-scale electrochromic smart windows are undergoing practical testing in buildings [3, 4].

An electrochromic device embodies a number of superimposed layers on a transparent substrate or between two transparent substrates, and optical transmittance is altered when an electrical potential is applied so that

charge is shuttled between layers serving in the same way as anodes and cathodes in an electrical battery. One approach with a five-layer construction in between two polyester foils (denoted 1) suspended in the air gap of a double-glazed window is shown in Fig. 1. This specific design uses cathodically coloring tungsten oxide (3) and anodically coloring nickel oxide (5) joined by an ion-conducting electrolytic laminate (4). A potential of a few volts, preferably supplied by solar cells, is applied between transparent and electrically conducting layers of  $\text{In}_2\text{O}_3:\text{Sn}$  (known as ITO; denoted 2) on the polyester. The spectral transmittance of this device in fully colored and bleached states is shown in Fig. 2; the luminous transmittance – obtained by integration over the eye's sensitivity curve – lies between 74 and 7%. Devices of a similar type, with films of tungsten oxide and nickel oxide operating in concert, have been subject to several recent investigations [5, 6, 7, 8, 9, 10, 11].

This paper discusses three different aspects of electrochromic smart windows of the type illustrated in Fig. 1. The role of energy efficiency is considered and it is shown that a systemic approach, accounting for the physical presence of persons, can yield large savings in the energy for space cooling [12, 13]. The possibility of removing a fundamental cause of electrochemical degradation – caused by the fact that the electrolytic laminate bounds on two different materials – by involving layers providing chemical compatibility [11] is discussed. The ozone exposure of nickel oxide as a step towards cheap manufacturing technology [14] is also treated.

### Energy efficiency: a systemic approach

This section provides a background to, and justification for, research on and development of architectural smart windows. We first note that buildings have windows to allow the occupants visual contact with their surroundings and to provide daylight. From an energy perspective, the window is problematic, though, and it normally

Presented at the Regional Seminar on Solid-State Ionics, Jūrmala, Latvia, 22–26 September 2001

A. Azens · C.G. Granqvist (✉)  
Department of Materials Science,  
The Ångström Laboratory, Uppsala University,  
P.O. Box 534, 751 21 Uppsala, Sweden  
E-mail: claes-goran.granqvist@angstrom.uu.se

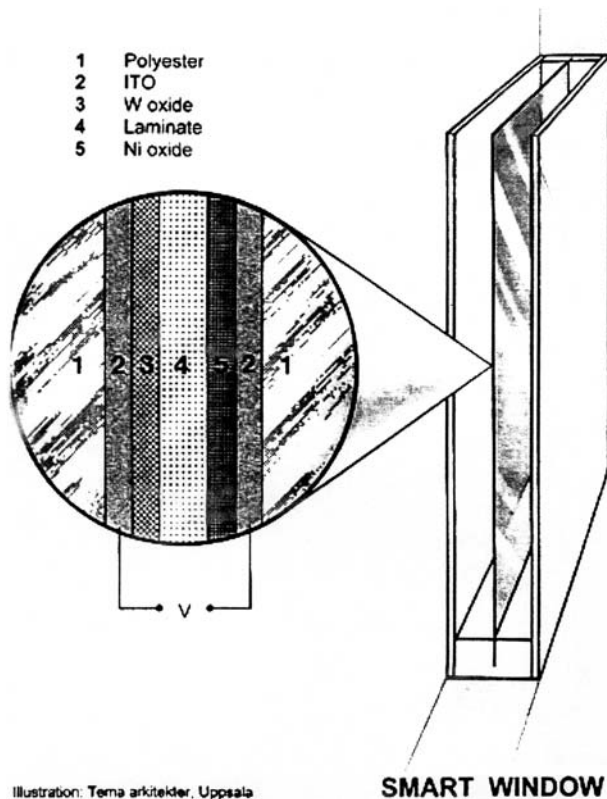


**Fig. 1** Conceptual smart window including laminated and coated plastic foil suspended between two glass panes. The window also includes a coating with low thermal emittance – prepared using known technology – whose role is to prevent the energy absorbed in the foil from being radiated into the room (not shown)

either lets in too much energy, so cooling is required to create a good indoor climate, or it lets out too much energy, so heating is needed. In modern commercial buildings, the problem of excessive heating normally dominates, and in the following we only consider cooled buildings.

There are numerous measures to avoid overheating by too much solar energy entering through windows, with blinds, awnings, and shutters having been used for long times. Multiple glazing diminishes heat transfer across the window aperture. Also the glass itself can be modified, normally by a “solar control” coating based on silver, which reflects part of the infrared solar radiation [15, 16]. Nevertheless, cooling is a problem – and it is aggravated by the increased use of personal computers and other office machines – so electrical power used in providing cooling now dominates the utilities’ peak loads in several parts of the world. It should also be emphasized that efficient solar control tends to lower visual transparency, thus compromising the windows’ primary function: that of allowing unmitigated visual contact with the ambience.

Smart windows are able to yield energy efficiency as well as comfort for the users of the building. The comfort issue is obvious since glare and thermal loads can be lessened at will. The energy efficiency has been harder to

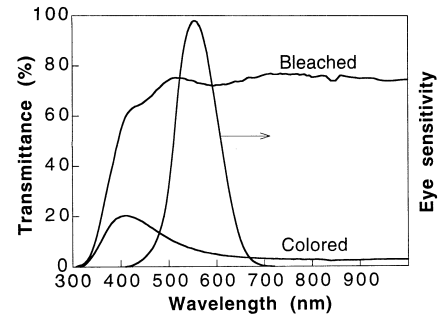


**Fig. 2** Spectral transmittance of an electrochromic foil in fully darkened and bleached states. Also shown is the sensitivity of the human eye. The visible transmittance is 73.5/7.1% in the bleached/colored state

come to grips with. Earlier studies [17] indicated some modest energy savings; the expected influence of the specific control strategy was large. We believe that this previous work did not consider what is likely to be the most important control strategy: to have the windows in a room in their dark state when no one is present and to have them transparent – according to individual choice – when the room is in use [12, 13, 18].

Quantitative energy savings can be estimated very simply. We take the solar energy density falling onto a window to be 1000 kWh/m<sup>2</sup>yr. This is regarded as a typical number for a south-facing window, and more correct values for south-facing/north-facing/horizontal surfaces would be 850/350/920, 1,400/450/1,700, and 1,100/560/1,800 kWh/m<sup>2</sup>yr for Stockholm (Sweden), Denver (USA), and Miami (USA). Half of the considered energy, 500 kWh/m<sup>2</sup>yr, is visible light; we only include this latter value for the smart windows, since the infrared radiation, in principle, can be intercepted by known, static technology. Taking the window to vary the transmittance between 7 and 75%, consistently with the data in Fig. 2, the energy saving inherent in the controllability is 340 kWh/m<sup>2</sup>yr, i.e., this is the difference between having the window in its darkest state and in its fully bleached state. The important question is then when the window should be dark and when should it be transparent. With physical presence as the overriding control strategy, one needs to contemplate when a typical room in a cooled (commercial) building is used – or rather the fraction of the solar energy which enters a typical room when someone is present. Considering that the room is expected to be empty during holidays, weekends, early mornings and late afternoons (when the sun is low), we believe that 50% represents a conservative estimate of the relative fraction of solar energy that enters a typical room when it is unoccupied. A minimum value for the energy saving is then 170 kWh/m<sup>2</sup>yr. In a real case, the smart window would not be fully transparent during at least some of the time it is used, so the energy savings would in fact be larger. Lower lighting energy is expected as well [19].

The energy savings may be appreciated by a simple analogy. Replacing the window aperture with a solar cell

module – assuming today’s best thin film solar cells with about 17% efficiency [20] – will generate 170 kWh/m<sup>2</sup>yr under the given conditions. The energy saving implied in smart windows is then the same as the electrical energy generated by the solar cell module in the same position. The analogy presumes air conditioning powered by electricity generated with a coefficient of performance of unity, as is commonly used in national scenarios for electricity generation. It should be noted that the analysis here gives a baseline for assessing energy efficiency rather than quantitative data for any particular building. A more refined analysis can follow along the lines given elsewhere [18].

### Durability: the case of six-layer devices

Electrochromic smart windows must function for long times. One major durability problem ensues from the incompatibility between the centrally positioned electrolytic layer and the adjoining two films, being tungsten oxide and nickel oxide according to the design in Fig. 1. Thus tungsten oxide is stable in a moderately acidic environment, whereas it is rapidly dissolved in a basic electrolyte. On the other hand nickel oxide is stable in a basic environment, but unstable in an acidic one. A possible solution to this dichotomous problem is to involve an additional protective layer [21], and it is shown later that stability can be accomplished by putting a layer of tungsten oxide on top of the nickel oxide counterelectrode. It should be stressed that the approach relies on the fundamental energetics of the multilayer structure and is not a trivial consequence of having a thin – and hence only weakly coloring – surface layer.

The six-layer design is depicted in the upper part of Fig. 3, where it is emphasized that the tungsten oxide films have two different functions: being protective of the underlying film, and exhibiting electrochromic properties. The use of a protective tungsten oxide film is suitable for devices with acidic electrolytes. The lower parts of Fig. 3 delineate highly schematic electron density-of-states (DOS) diagrams. The nickel oxide film can be represented as a Mott insulator [22] with a wide band gap due to the large correlation between the Ni 3*d* electrons [23]. Complications may arise because the films are likely to be hydrous [24]. In the bleached state, the Fermi energy,  $E_F$ , is expected to lie slightly above the valence band edge [25]. For tungsten oxide,  $E_F$  lies in the band gap separating a valence band dominated by O 2*p* states from a conduction band dominated by W 5*d* states [23].

When a voltage,  $U_{col}$ , is applied between the nickel oxide and tungsten oxide films – as indicated in the right-hand part of Fig. 3 – their Fermi levels are separated. Electrons enter the W 5*d* states, where they may cause strong polaron absorption [2, 26] provided that the tungsten oxide film is heavily disordered. A corresponding charge is subtracted from the top of the valence band of the nickel oxide film, thereby rendering this material absorbing by a mechanism that appears to

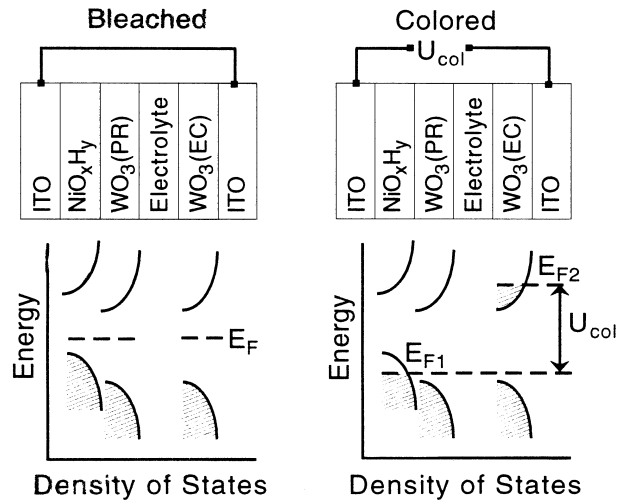


**Fig. 3** Schematic electron density-of-states diagrams for electrochromic, EC, multilayer design. The materials include In<sub>2</sub>O<sub>3</sub>:Sn (ITO), nickel oxide (presumably hydrous), tungsten oxide (also presumably hydrous) prepared so that the EC and chemically protective (PR) properties are emphasized, and an electrolyte. The Fermi energy is denoted  $E_F$ , with  $E_{F1}$  and  $E_{F2}$  pertaining to the case of an applied potential,  $U_{col}$ . Filled states are denoted by *shadings*

be non-polaronic but is not known in detail [27]. Hence the initially transparent device turns absorbing by a combination of anodic electrochromism in nickel oxide and cathodic electrochromism in tungsten oxide.

The relative energies of the DOS for the two types of films can be inferred by additional arguments. Thus, if an absorbing device combining nickel oxide and tungsten oxide is electrically shorted it turns transparent, implying that the bottom of the conduction band of tungsten oxide lies at a higher energy than the top of the valence band for nickel oxide. Figure 3 assumes rigid-band behavior for the DOS, which appears well founded for tungsten oxide [23] but is less established for nickel oxide. It should be stressed that the protective tungsten oxide layer in the device is always transparent and does not contribute to device coloration at any stage, although it is capable of imparting chemically desirable surface properties to the anodically coloring electrochromic nickel oxide film.

Experimental studies were performed on devices whose principles are illustrated in the upper part of Fig. 3. Films were produced by reactive direct current magnetron sputtering onto unheated substrates from metallic targets of W and Ni in a mixture of Ar, O<sub>2</sub>, and, in some cases, H<sub>2</sub>. Specific experimental data can be found in Ref. [11]. Electrochromic tungsten oxide was deposited at a high sputtering pressure, while a low pressure – giving dense films – was found to be suitable for protective layer deposition. Electrochemical characterization of the tungsten oxide films was performed by cyclic voltammetry in an electrolyte of lithium perchlorate in propylene carbonate. Typical data for 300-nm-thick films are shown in Fig. 4a. The porous

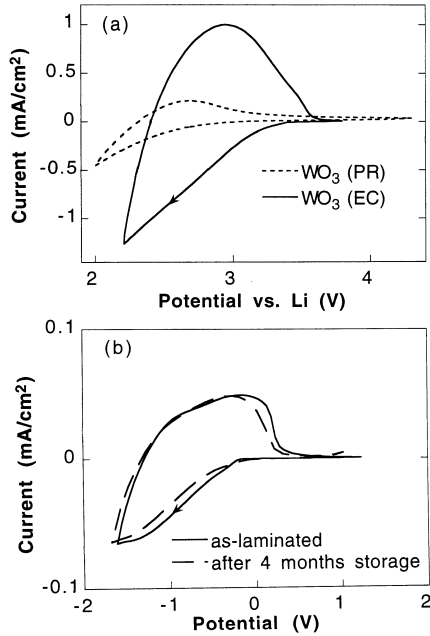


**Fig. 4** Cyclic voltammograms for **a** tungsten oxide sputter deposited at different gas pressures to prepare films with suitable protective, PR, and electrochromic, EC, qualities and **b** an ITO/nickel oxide/tungsten oxide/ZrP electrolyte/tungsten oxide/ITO device in an as-prepared state and after extended storage. The voltage was swept at 50 mV/s. Arrows denote the sweep direction

electrochromic film yields a performance that is typical for electrochromic tungsten oxide [2, 26]. The relatively compact nature of the protective film, however, leads to slow ion intercalation/deintercalation and small charge exchange.

Devices of the types illustrated in Fig. 3 were constructed and subjected to durability tests. Specifically, the acidic electrolyte was a 50- $\mu$ m-thick transparent proton-conducting ZrP-based layer [28]. Device assembly took place in air, and sealing employed a two-component epoxy glue. Voltammograms taken on an as-laminated device and after four months of storage are shown in Fig. 4b. In a similar device without a protective layer, the lifetime of the nickel oxide film was of the

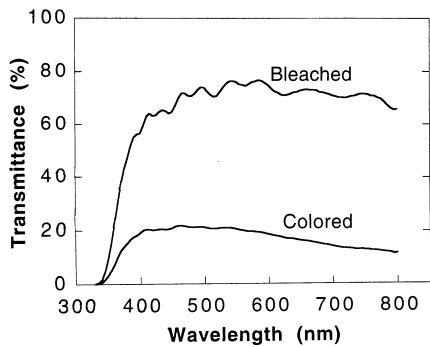


**Fig. 5** Spectral transmittance for an ITO/nickel oxide/tungsten oxide/ZrP electrolyte/tungsten oxide/ITO device in fully colored and bleached states

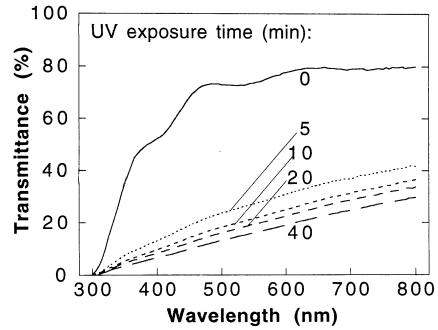


**Fig. 6** Spectral transmittance of a nickel oxide film exposed to ozone for the times shown

order of a few seconds. No features in the data can be clearly assigned to the introduction of the protective-type tungsten oxide. The spectral optical properties for the device in fully bleached and colored states, corresponding to the potentials  $U_{col} = 1.9$  V and  $U_{bl} = -0.2$  V, respectively, are illustrated in Fig. 5. Clearly the electrochromism is pronounced, with the luminous transmittance going from 76 to 21%. Figures 4b and 5 refer to a device employing a 300-nm-thick protective layer. In general, the optimum thickness and density of the protective layer varies depending on the acidity and viscosity of the electrolyte.

**Device manufacturability: ozone treatment of nickel oxide**

An electrochromic smart window, such as the one depicted in Fig. 1, must be manufactured by techniques that are both efficient and inexpensive. One potentially cumbersome step involves precharging the individual layers of the device so that it can be altered between fully transparent and dark states by a low voltage. As shown in the following, an initial charge deficit in nickel oxide films can be achieved by a simple ozone treatment [14].

Nickel oxide films were made in the same way as for the studies reported in the previous section. Initially

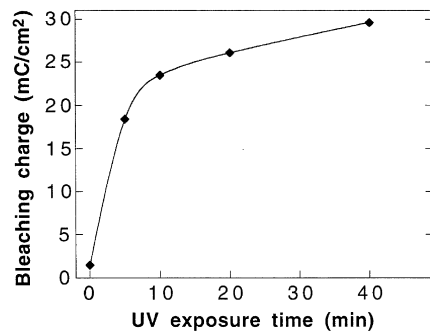


**Fig. 7** Time for coloration by UV exposure in air versus charge density for subsequent full electrochemical bleaching of nickel oxide films

transparent films were colored by ultraviolet, UV, irradiation in an ozone photoreactor operated in air. Specifically, Hg lamps provided a nominal irradiation intensity of  $15 \text{ mW/cm}^2$  at a wavelength of 245 nm and an intensity of  $1.5 \text{ mW/cm}^2$  at 185 nm. The ozone concentration was 50 ppm under steady-state operation. The spectrophotometrically measured transmittance is reported in Fig. 6 for a 220-nm-thick film exposed to UV radiation for up to 40 min. Irradiation for a few minutes diminished the luminous transmittance by some 50%, and a further decrease of the transmittance took place for extended exposures. UV irradiation in the absence of oxygen, on the other hand, was able to provide some bleaching of as-deposited nickel oxide films, which tend to be dark especially if they are not made by sputtering in the presence of hydrogen [29].

The coloration upon ozone exposure corresponds to a well defined amount of charge density extracted from the nickel oxide film. This relationship forms the basis of electrochromism and is often expressed in terms of a coloration efficiency [2]. The amount of charge density to bleach the film was determined electrochemically. To that end, the colored film was immersed in an electrolyte of potassium hydroxide and charge was introduced in the film by use of voltammetry. Optical measurements were performed in order to determine when a fully transparent state was reached. The UV exposure time needed to achieve a certain degree of coloration and the charge insertion required to regain a fully transparent (bleached) state is illustrated in Fig. 7. It appears that a bleaching charge of about  $20 \text{ mC/cm}^2$  corresponds to UV-induced coloration for under 10 min., and that a bleaching charge of about  $30 \text{ mC/cm}^2$  is needed after UV coloration for an extended period of time.

The practical operation of devices such as those in Fig. 1 relies on inserting and extracting a charge density of the order of  $10\text{--}20 \text{ mC/cm}^2$  between the two kinds of films in order to effect an optical modulation according to Fig. 2. This is then the charge deficit that should exist in the nickel oxide film that is joined to the tungsten oxide film being colored by charge insertion to the same extent using one of several known techniques [2] including sputtering in the presence of hydrogen [30]. These arguments hence lead us to conclude that the novel technique employing ozone coloration of nickel oxide based films offers an efficient way of preparing the counterelectrode in an electrochromic device of a preferred design for assembly.

**Acknowledgements** A.A. thanks the Swedish Foundation for Strategic Environmental Research and the National Energy Administration of Sweden for financial support.

## References

1. Campagno A (1999) *Intelligente Glasfassaden/Intelligent glass façades*. 4th edn. Birkhäuser, Basel
2. Granqvist CG (1995) *Handbook of inorganic electrochromic materials*. Elsevier, Amsterdam
3. Anonymous (2001) *Int Glass Rev* 1:42
4. Lampert CM (2001) *Proc Soc Photo-Opt Instrum Eng* 4458:95
5. Lee SH, Joo SK (1995) *Solar Energy Mater Solar Cells* 39:155
6. Mathew JGH, Sapers SP, Cumbo MJ, O'Brien NA, Sargent RB, Raksha VP, Lahaderne RB, Hichwa BP (1997) *J Non-Cryst Solids* 218:342
7. Azens A, Kullman L, Vaivars G, Nordborg H, Granqvist CG (1998) *Solid State Ionics* 113–115:449
8. Lechner R, Thomas LK (1998) *Solar Energy Mater Solar Cells* 54:139
9. Nagai J, McMeeking GD, Saitoh Y (1999) *Solar Energy Mater Solar Cells* 56:309
10. Karlsson J, Roos A, (2000) *Solar Energy* 68:493
11. Azens A, Vaivars G, Veszelei M, Kullman L, Granqvist CG (2001) *J Appl Phys* 89:7885
12. Granqvist CG (2001) *Int Glass Rev* 2:67
13. Granqvist CG (2001) *Interface* 3:18
14. Azens A, Kullman L, Granqvist CG (2002) *Solar Energy Mater Solar Cells* (to be published)
15. Granqvist CG (1991) In: Granqvist CG (ed) *Materials science for solar energy conversion systems*. Pergamon, Oxford, pp 106–167
16. Hollands KGT, Wright JL, Granqvist CG (2001) In: Gordon J (ed) *Solar energy: The state of the art*. James & James, London, pp 29–107
17. Sullivan R, Rubin M, Selkowitz S (1996) Lawrence Berkley National Laboratory Report LBNL-39905
18. Karlsson J (2001) In: Lamberts R, Negrão C, Hensen J (eds) *Proceedings of the seventh conference of the International Building Performance Simulation Association*, Rio de Janeiro, Brazil, August 13–15. pp 119–206
19. Lee ES, Di Bartolomeo DL (2002) *Solar Energy Mater Solar Cells* 71:465
20. Kessler J, Wennerberg J, Bodegård M, Stolt L (2001) (to be published)
21. Shen PK, Huang HT, Tseung ACC (1992) *J Mater Chem* 2:479
22. Mott NF (1990) *Metal-insulator transitions*, 2nd edn. Taylor & Francis, London
23. Hjelm A, Granqvist CG, Wills JM (1996) *Phys Rev B* 54:2436
24. Svensson JSEM, Granqvist CG (1986) *Appl Phys Lett* 49:1566
25. Hüfner S (1994) *Adv Phys* 43:183
26. Granqvist CG (2000) *Solar Energy Mater Solar Cells* 60:201
27. Nilsson TMJ, Niklasson GA (1990) *Proc Soc Photo-Opt Instrum Eng* 1272:129
28. Vaivars G, Azens A, Granqvist CG (1999) *Solid State Ionics* 119:269
29. Estrada W, Andersson AM, Granqvist CG (1988) *J Appl Phys* 64:3678
30. Giri AP, Messier R, (1984) *Mater Res Soc Symp Proc* 24:221